euspen's 22nd International Conference & Exhibition, Geneva, CH, May/June 2022
www.euspen.eu

Optimization of fast tool servo diamond turning for enhancing geometrical accuracy and surface quality of freeform optics

Lin Zhang, Yusuke Sato, Jiwang Yan*

Department of Mechanical Engineering, Keio University, 3-14-1, Hiyoshi, Kohoku-ku, Yokohama, 223-8522, Japan

Corresponding author: yan@mech.keio.ac.jp

Abstract
Fast tool servo (FTS) diamond turning is a promising technique for high-precision generation of freeform optics with remarkable efficiency. However, the conventional constant scheme for control point sampling fails to consider the surface variation, which might lose some details of the surface profile and result in low form accuracy and non-uniform surface quality. Facing this issue, this manuscript proposes a novel optimization method for control points sampling, which restrains the deviations and contains as much of the surface details. In the optimization method, the sampling intervals between two adjacent control points are actively adjusted to adapt the surface variation of the desired surface. By adopting this method, the sampling induced interpolation error between the control points is restrained within the tolerance and eliminates lack/over-definition of control points in the machining area. The feasibility of the proposed optimization method is demonstrated by both theoretical prediction and fabrication experiment of sinusoid freeform surface. Compared with the conventional sampling method, both the predicted and measured form error of the proposed method are remarkably reduced about 35 % with the same amount of control points. This technique provides a new route to sampling control points in FTS diamond turning to achieve high accuracy and flexible fabrication of freeform surface machining.

Keywords: Fast tool servo, optimization sampling method, control points, desired tolerance

1. Introduction

Freeform optical surface, designed with little to no symmetry, is generally regarded as a disruptive evolution of optical systems, since it constitutes a powerful tool offering the possibility to enhance the optical performance or compact the volume of optical systems required by conventional designs, or a combination of these two attractive features [1]. Recently, the increasing applications of freeform optics in imaging and non-imaging optical systems stimulate demands on the fabrication of intricate surfaces with high accuarcy and efficiency [2]. Fast tool servo (FTS) diamond turning is regarded as one of the most promising techniques due to its superior capability on sub-micro form error, nanoscale roughness and high machining efficiency. Recently, massive effort has been made to obtain the optimal processing conditions and improve the accuarcy and efficiency, including the optimization machining parameters [2-3], determination of toolpath [4-5], and static and dynamic motion induced error compensation [4, 6]. With the aid of these techniques, the form accuracy and surface integrity in FTS diamond turning have been remarkably improved on a wide range of engineering materials.

In diamond turning process, the relative motion between the diamond tool and the workpiece is utilized to carve out the shape of the desired surface. Different from the conventional slow tool servo (STS) diamond turning, in which the motions of the axes are fully controlled by the machine tool and the tool position is determined by linear-interpolation with the adjacent control points on a spiral toolpath, the separated FTS adopts an independent system with a novel strategy to drive the diamond tool for flexibility and fast-response, as shown in Fig. 1. As an independent driven unit, the FTS controller is equipped with a signal amplifier and a successive of control units, which are employed to collect the notification and feedback, adjust signal deviation and enable the diamond tool. Besides, the unidirectional communication between the machine tool and the FTS controller further enhances the requirements on processing capacity and rapid response. In general, the tool position determined by the separate FTS controller is based on two-dimensional (2D) interpolation utilizing the adjacent control points. Deriving from this, the layout and storage of control points in the FTS controller have to be satisfied with at least two pivotal requirements: (a) the amount of the control points should be limited to be easily operated by the FTS control system; and (b) the control points should be well-organized for fast positioning and easy search.

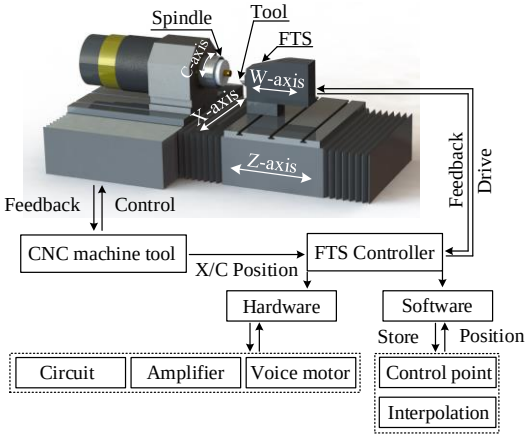

Figure 1. The hardware configuration and control flow of the independent FTS diamond turning.

Generally, two kinds of sampling methods are mainly used in F/STS diamond turning. One is the constant-angle sampling strategy (CASS) and the other one is the constant-arc-length sampling (CALS). Considering the requirement on data order, CASS is a more common method. The interpolation error is highly dependent on the distance between the cutting point and

the center point due to the increasing arc-length between two adjacent control points. To guarantee sufficient control points at the largest radius, angular subdivision should be conducted, which, in turn, results in over-defined control points concentrated around the center point, greatly increasing machining cycle time and program file size. In addition, it will significantly slow down the response of the control system due to the intricate interpolation and servo time, which easily leads to the asynchronization of the physical motions of the slides. To reduce the number of control points, achieve uniform sampling and rapid response, in STS or conventional FTS diamond turning, the CALS as well as the hybrid sampling strategy combining the CASS and CALS were proposed [7]. However, these strategies were no long suitable for the independent FTS controller.

Another important factor in the form error is due to the surface profile. For the freeform optics, the surface variation may lead to remarkable interpolation error with respect to different cutting points. Thus, the CASS or CALS sampling methods, regardless of surface variation, inevitably result in heterogeneous distribution of interpolation errors on the final machined surface. Recently, to improve the quality of F/STS machined freeform surfaces, an adaptive diamond turning method, fully considering the side-feeding and forward sampling of control points to fit the surface variation, was proposed and demonstrated [5]. Although the adaptive diamond turning may be superior in generating more accurate surfaces, the computation load is significantly increased, compared with the common CASS and CALS sampling methods. In addition, this method, re-locating the control points from the spiral pattern, induces high-frequency vibration in x-axis, which might not be suitable for most commercial one-dimensional (1D) FTS.

Facing this issue, a novel sampling strategy should be introduced to satisfy the requirements of the independent FTS controller. Since the constant stepover without consideration of surface variation may not be suitable for freeform optics, especially for some surfaces with significant fluctuation, in this research, a variable stepover along the cutting-froward and side-feeding directions is introduced into control points sampling to improve the surface accuracy. Then, the adaptive control point sampling (ACPS) strategy is proposed with consideration of interpolation error corresponding the surface profile variation. To demonstrate the feasibility and superiority of this method, both numerical simulation and diamond turning experiment were conducted. The present study provides a new route to improve the surface form accuracy and machining efficiency in freeform optics fabrication.

2. Methodology

2.1. FTS control system and strategy

In F/STS diamond turning, the turning operation is generally conducted in the cylindrical coordinate system (ρ, θ, z), in which the diamond tool follows a spiral motion. The relative motion along the tangent line is referred as cutting forward direction, while the polar axis directions are regarded as side-feeding direction. The servo motion along the z-axis is utilized to carve out the contour of the disgined surface. For the conventional STS, the spatial three coordinates, including ρ, θ and z, are determined in toolpath generation and the motions of x-, y- and z-axes follow each instruction to complete the whole machining process. However, in the separated FTS diamond turning, the control strategy is completely different from that in the conventional STS diamond turning, since the FTS controller has gained enhanced capability to achieve remarkable processing capability and ultra-fast response. Thus, in the FTS controller, a complete description of the machined surface profile, consisted with control points or functions, is elaborately organized and stored, rather than the spiral pattern.

In order to distinguish the motions of the machine tool and the FTS unit in z-axis, the motion of FTS in z-axis is usually called w-axis. In FTS turning operation, the real-time x-/c-axes positions are monitored by the grating encoders equipped on the machine tool, which are immediately sent to the FTS controller. The x-/c-axes positions are employed as input for the FTS command generator, which is regarded as the reference location for searching the nearby control points. In general, there are mainly two kinds of sampling methods for locating control points, which take both accuracy and availability into consideration, namely ring method and mesh method, as shown in Fig. 2. For the ring method, as shown in Fig. 2(a), the control points are placed on a series of concentric circles with a constant pitch between them. On each circle, the control points are uniformly distributed along the arc with a constant angle Δθ. The adjacent concentric circles pitch Δρ and the constant-angle Δθ are two geometrical parameters for control point sampling. Similarly, the control points generated by mesh method form a rectangular pattern, where Δx and Δy are the pitches between two adjacent points along the x- and y-axes. After the nearby control points are found out, the tool position is determined by 2D interpolation, which is further adjusted and amplified by the PID controller to drive the w-axis.

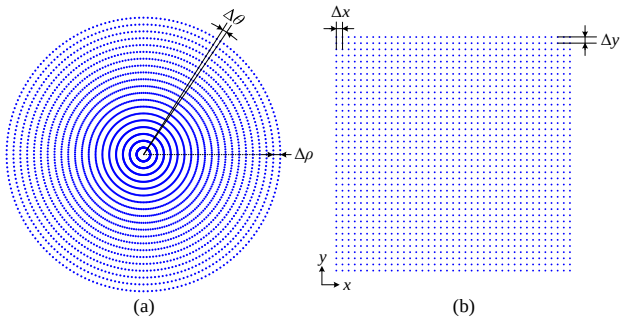

Figure 2. Schematic diagram of layouts of control points generated by (a) ring method, and (b) mesh method.

2.2. Optimization method for the independent FTS

For a specified freeform surface with determined diamond tool geometry, the primary controllable factors that governing the final surface accuracy are the interpolation method, sampling density and the side-feeding induced residual tool marks, as illustrated in Fig. 3. As an important section in final surface form error, the interpolation method does not exert the same independence as other factors, which commonly influence the form accuracy with surface profile variation and control point density. Along the forward cutting direction as shown in Fig. 3(a), the interpolation error between two adjacent control points will lead to two kinds of interpolation errors in term of the positive/negative of the deviations: (a) the convexity induced over-cutting effect (negative), and (b) the concavity induced less-cutting effect (positive). Although some improved interpolation methods could effectively minimize the deviations, the computation load is increased by several order than the most commonly used linear method [8]. On the other hand, the side-feeding motion will always lead to positive tool residual tool marks, as shown in Fig. 3(b).

In the FTS turning, the side-feeding motion induced form error can be eliminated by decreasing the motion rate in x-axis, which is thought to be un-acceptable in conventional STS due to the efficiency. However, since the spindle speed in FTS (100~600 rpm) is usually tens/hundreds of times faster than that used in the conventional STS (5~30 rpm), the decrased motion rate in x-axis does not lead to significant reduction on machining efficiency. Thus, the sampling interval on the whole machined surface should be carefully adjusted to cover each micro-feature

on the machined surface. Thus, the constant interval between the adjacent control point is no longer suitable for intricated surface profiles, especially large-aperture freeform optics. In the ACPS, the sampling interval, including the ring method and mesh method, is deliberately determined to adapt to surface variations. By carefully adjusting the control points, the interpolation error is always limited within the acceptable range on the machined surface, which can realize the full potentials of each control point. Thus, a much larger sampling interval can be adopted with slight curvature variation and vice versa. Through this method, the optimization can remarkably cut down the volume of the control points when comparing the conventional sampling method with the comparable surface accuracy.

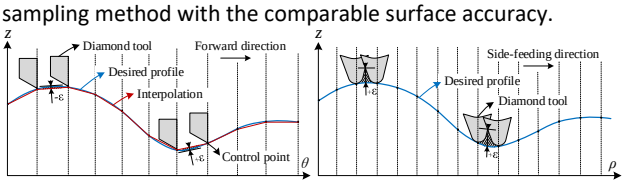

Figure 3. Schematic diagram of form error generation in (a) the forward cutting direction, and (b) the side-feeding direction.

2.3. Control point determination

As mentioned above, in both ring pattern and mesh pattern, two geometrical parameters are needed to be optimized to simultaneously satisfy the form error tolerance along two directions. Since the ACPS will not change the original organization of the control points, *i.e*. equivalent control points per revolution, the optimization process for the two parameters are divided into two steps to enhance the arithmetic robustness. The next part takes the mesh sampling pattern as an example. Since the two geometrical parameters (Δx and Δy) have the equivalence property, the order of optimization does not matter. Thus, in the following section, the optimization is conducted with Δx and Δy consecutively.

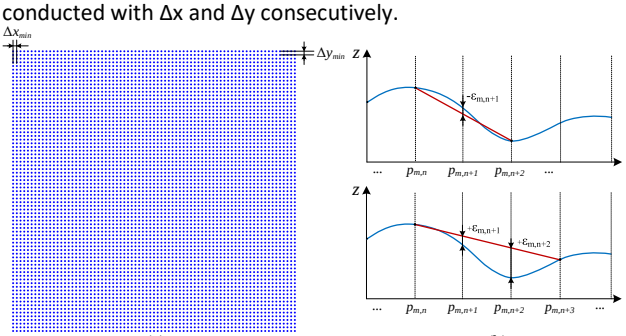

Figure 4. Schematic diagrams of optimization process (a) initialization of control point, and (b) determination principle.

At initial stage, the machine area is homogeneously divided in small squares with Δx_{min} and Δy_{min} along x- and y-axes, which are treated as the smallest unit for Δx and Δy, as shown in Fig. 4(a). The initial sampling control points are marked with the number of row and column and the desired surface can be express as $z_{m,n} = f(x_{m,n}, y_{m,n})$. Then, the optimization for Δx is initialized from $p_{1,1}$ to $p_{m,1}$, as shown in Fig. 4(b). For instance, the control points $p_{m,n}$ and $p_{m,n+2}$ are selected from the sequence. Based on the 1D linear interpolation, the predicted value $z_{m,n+1}'$ at the position of $x_{m,n+1}$ can be obtained and the deviation between the actual value $z_{m,n+1}$ and $z_{m,n+1}'$ can be calculated as $\varepsilon_{m,n+1} = | z_{m,n+1} - z_{m,n+1}' |$. If the obtained deviation $\varepsilon_{m,n+1}$ is larger than the acceptable tolerance ε_x, the initial point $p_{m,n+1}$ is chosen as the determined control point, which is further utilized as the initial point to determine the next control point. On the other case, when the obtained deviation $\varepsilon_{m,n+1}$ is less than the acceptable tolerance ε_x, the next point ($z_{m,n+3}$) along the m^{th} row is abstracted and calculated the deviations at the positions of $x_{m,n+1}$ and $x_{m,n+2}$. If either of the calculated deviations ($x_{m,n+1}$, $x_{m,n+2}$) fails to satisfy the requirement on tolerance, the control point is set at the point of $p_{m,n+2}$. However, considering the data organization, the minimum Δx should be selected from the columns ($\Delta x_{m,n} = \min \Delta x_{1\sim max,n}$). Similar optimization operation is conducted along the y-axis to determine the appropriate sampling interval Δy based on the surface profile.

2.4. Experimental setup and conditions

To characterize the ACTS method, a typical sinusoidal micro-structured surface was utilized for demonstration by both numerical prediction and experiment. The surface profile can be mathematically described as $z(x,y) = A\sin(2\pi f_x x) + B\sin(2\pi f_y y)$. The amplitude and the spatial frequency were set as A = B = 0.5 μm and $f_x = f_y = 10$ mm^{-1}. The side-feeding rate was set as $f_v = 5$ μm/rev and 1 μm/rev for the rough and final diamond turning operations. The tool used in the experiment was a commercial natural single-crystalline diamond tool with nose radius of R_t = 0.083 mm, rake angle of 0° and clearance angle of 8°.

The diamond turning experiments were conducted on a multi-axis ultra-precision lathe Nanoform X (AMETEK Precitech Inc., USA). The hardware configuration of the setup is shown in Fig. 5(a). After machining, the machined surface was cleaned by acetone and alcohol to remove the attached chips. The optical image of the machined surface is shown in Fig. 5(b). The optical profilometer (Zygo Nexview, AMETEK Zygo Corp., USA) was employed to capture the micro-morphologies of the machined surface, which was further introduced into the mathematical software for further analysis.

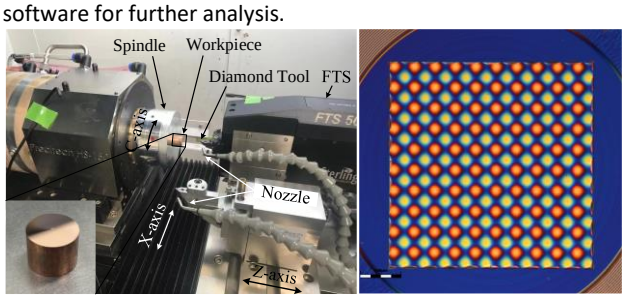

Figure 5. (a) Hardware configuration of the FTS diamond turning and (b) the optical images of the demonstration optical surface.

3. Result and discussion

3.1. Theoretical prediction of control point sampling

In the ACPS optimization, the tolerances of the interpolation errors and initial minimum step were set as $\varepsilon_x = \varepsilon_y$ = 10 nm and $\Delta x_{min} = \Delta y_{min}$ = 50 nm, which can be fulfilled the requirements for most of the optical applications. The ACPS control point pattern with the corresponding micro-structure surface is illustrated in Fig. 6(a). In order to have intuitive comparison, the conventional equidistant mesh sampling method, with the same number of control point, is further illustrated in Fig. 6(b). To get a better description of the features of the sampling, the projected control point clouds for conventional and ACPS mesh sampling are shown in Fig. 6(c) and 6(d). Different from the control point pattern with constant interval in Fig. 6(c), the ASCS control point pattern, in Fig. 6(d), possesses variable sampling intervals, which are closely related with the variation of local surface variation.

3.2. Theoretical investigation of surface generation

To further investigate the feasibility of the proposed ACPS method, numerical prediction of the machined surface was conducted for both ACPS and conventional mesh sampling methods to determine the final surface form errors. By removing the desired surface profile, the error maps by numerical prediction for the ACPS method and conventional mesh method are illustrated in Fig. 7(a) and 7(b), respectively. From the results, the distribution of form error was highly dependent on the surface profile variation, concentrated near the concavity or convexity and illustrating non-uniform error distribution. To have a clear view of the error, the obtained error maps are

observed from xz-plane as shown in Fig. 7(c) and 7(d). By comparison, the form error on ACPS method surface was constrained in a narrow band within ±19.632 nm, while the form error by conventional mesh sampling approximately follows harmonic curves, covering within ±30.072 nm. This suggested that the ACPS method has largely reduced the surface error, which is about 65.3 % of the error by conventional sampling.

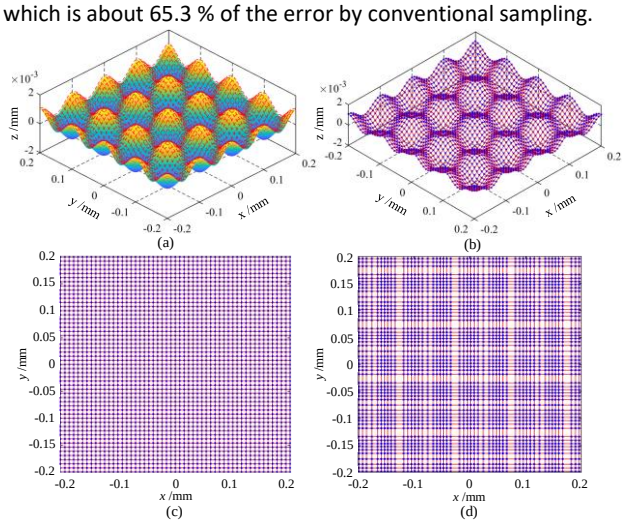

Figure 6. Schematic diamgram of (a) the demonstration surface and (b) the corresponding control points, (c) and (d) the projected conventional control points and the ACPS for the F/STS.

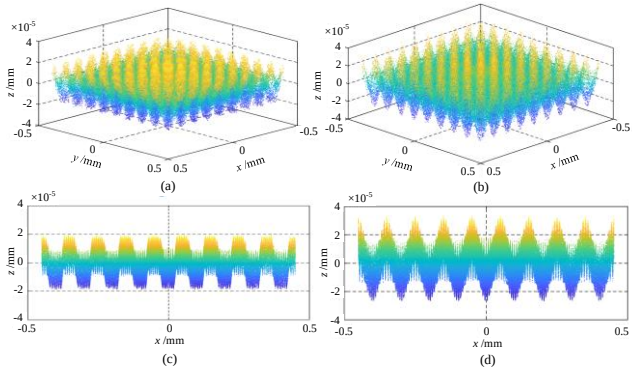

Figure 7. Theoretical prediction of the machined surface by (a) ACPS, and (b) conventional mesh sampling, and the corresponding error maps in xz-plane by (c) ACPS, and (d) conventional sampling.

3.3. Surface characterization and discussion

The obtained micro-morphologies of the machined surfaces by using ACPS and conventional mesh sampling method are captured and shown in Fig. 8(a) and 8(b). After removing the desired surface profile, the corresponding error maps are shown in Fig. 8(c) and 8(d). From the result, it is clear that significant reduction of form error is achieved on the machined surface with ACPS method, which well agree with the numerical prediction in Fig. 7(a). The error map obtained from the machined surface by conventional mesh sampling method involves remarkable concavity and convexity in Fig. 8(d), which was similar with the theoretical prediction result shown in Fig. 7(d). However, the measured PV-values results are larger than those of the numerical prediction. It might be due to the other potential factors affecting the final form error, such as tool shape error. Based on the above result, the feasibility of the ACPS method was demonstrated for achieving uniform surface quality and constraining form error. The comparison between two machined surfaces is listed in Table 1.

Table 1 Surface characteristics of the machined surfaces

	ACPS method	Conventional method
Number of control point	17161	
PV-value /nm	66.4545	106.5578
RMS /nm	11.0402	16.9140
Surface roughness S_a /nm	4.5	5.2

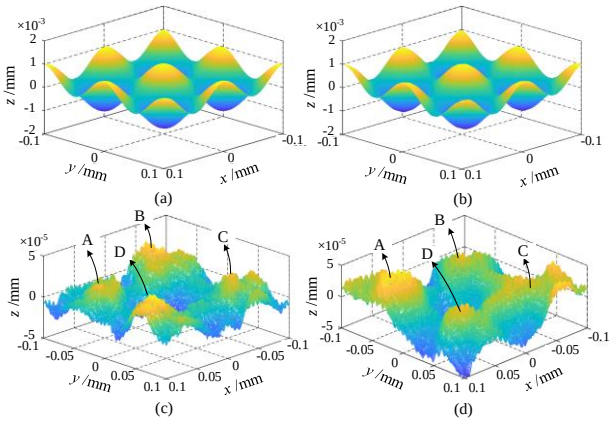

Figure 8. Measured machined surface by (a) ACPS, (b) conventional sampling, and the corresponding form error of the diamond turned surface obtained by (c) ACPS, and (d) conventional sampling method.

4. Conclusions

A novel ACSP method for FTS diamond turning is proposed for generation of intricated freeform optics to improve the form accuracy and enhance the efficiency simultaneously. Different from the conventional STS diamond turning, the control points on the machined area are sampled in concentric or mesh patterns. By computation of the interpolation error along both directions, the optimal sampling interval, adaptive to the surface profile variation, can be precisely determined. In addition, a theoretical comparison of the machined surface in both ACSP and conventional uniform sampling was conducted. The numerical results indicated that the ACSP can remarkably improve the surface form accuarcy and surface roughness with same amount of control points. Finally, cutting tests were conducted, which presented well agreement with the predicted results.

Acknowledgement

Lin Zhang is an International Research Fellow of the Japan Society for the Promotion of Science (JSPS) (ID No. is P 20368). This study has been financially supported by Grant-in-Aid for JSPS Fellows.

References

1. Zhang L, Naples N J, Zhou W, and Yi A Y 2019 Fabrication of infrared hexagonal microlens array by novel diamond turning method and precision glass molding *J. Micromech. Microeng.* **29** 65004
2. Yang F and Dai Y F 2010 Machining parameters selecting and optimization for fast tool servo considering the FTS dynamics *Advances in Optoelectronics and Micro/nano-optics* 1-5.
3. Yu D P, Wong Y S, and Hong G S 2011 Optimal selection of machining parameters for fast tool servo diamond turning Int. J. Adv. Manuf. Tech. **57** 85-99
4. Yu D P, Hong G S, and Wong Y S 2012 Profile error compensation in fast tool servo diamond turning of micro-structured surfaces *Int. J. Mach. Tool. Manu.* **52** 13-23
5. Zhu Z and To S 2015 Adaptive tool servo diamond turning for enhancing machining efficiency and surface quality of freeform optics Opt. Express **23** 20234-20248
6. Lu X and Trumper D L 2007 Spindle rotary position estimation for fast tool servo trajectory generation *Int. J. Mach. Tool. Manu.* **47** 1362-1367
7. Neo D W K, Kumar A S, and Rahman M 2014 A novel surface analytical model for cutting linearization error in fast tool/slow slide servo diamond turning *Precis. Eng*. **38** 849-860
8. Scheiding S, Yi A Y, Gebhardt A, Li L, Risse S, Eberhardt R, and Tünnermann A 2011 Freeform manufacturing of a microoptical lens array on a steep curved substrate by use of a voice coil fast tool servo *Opt. Express* **19** 23938-23951